J|A|C|S
ARTICLES
Published on Web 02/24/2007

Compound I of Nitric Oxide Synthase: The Active Site Protonation State

Kyung-Bin Cho, Etienne Derat,[#] and Sason Shaik*

Contribution from the Department of Organic Chemistry and the Lise Meitner-Minerva Center for Computational Quantum Chemistry, The Hebrew University of Jerusalem, 91904 Jerusalem, Israel

Received September 14, 2006; E-mail: sason@yfaat.ch.huji.ac.il

Abstract: A quantum mechanical/molecular mechanical (QM/MM) study of the formation of the elusive active species Compound I (Cpd I) of nitric oxide synthase (NOS) from the oxyferrous intermediate shows that two protons have to be provided to produce a reaction that is reasonably exothermic and that leads to the appearance of a radical on the tetrahydrobiopterin cofactor. Molecular dynamics and energy considerations show that a possible source of proton is the water H-bond chain formed from the surface to the active site, but that a water molecule by itself cannot be the source of the proton; an H_3O^+ species that is propagated along the chain is more likely. The QM/MM calculations demonstrate that Cpd I and H_2O are formed from the ferric−hydrogen peroxide complex in a unique heterolytic O−O cleavage mechanism. The properties of the so-formed Cpd I are compared with those of the known species of chloroperoxidase, and the geometry and spin densities are found to be compatible. The Mössbauer parameters are calculated and may serve as experimental probes in attempts to characterize NOS Cpd I.

Introduction

Nitric oxide synthase (NOS) catalyzes the conversion of L-arginine to L-citrulline and NO in two half-reactions (Scheme 1). In the first half-reaction,[1−6] L-arginine is converted to N^{ω}-hydroxy-L-arginine (NHA) upon consumption of O_2 and two electrons ultimately provided by NADPH. The second half-reaction converts NHA to L-citrulline and generates the physiologically important neurotransmitter substance nitric oxide (NO), again with consumption of O_2 but this time with only one-electron reduction. Both half-reactions occur in the presence of a tetrahydrobiopterin (H_4B) cofactor, which loses an electron and is converted to a radical in the process and is known to be kinetically coupled to the decay of the peroxo $Fe^{III}-O_2^-$ intermediate species.[7−9] These results are consistent with an electron transfer occurring from H_4B to the ligated O_2 moiety, to form $Fe^{III}-O_2^{2-}$. To date, while the $Fe^{III}-O_2^-$ species has been experimentally identified within a working cycle,[8,9] the successive one-electron-reduced species $Fe^{III}-O_2^{2-}$ has only been detected under cryogenic conditions, after cryo-reduction using γ-irradiation to add an additional electron into the system.[10] The details of the ensuing NOS reaction mechanism are, however, still unclear. For instance, no ferric−hydroperoxy Compound 0 species ($Fe^{III}-OOH$, Cpd 0) could be detected using cryo-annealing EPR and ENDOR spectroscopies, which is in sharp contrast to other heme enzymes like P450 and heme oxygenase.[10] Also, due to the similarity of NOS to cytochrome P450 systems, the current consensus is that the oxidation of Arg is caused by the high-valent iron−oxo species, Compound I (Cpd I), which is known to be present in many other heme-containing systems.[10−17] However, the existence of such a

Scheme 1. The Two NOS Half-Reactions

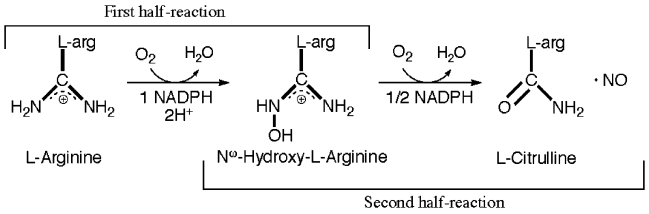

[#] Current address: Laboratoire de Chimie Organique (UMR 7611 CNRS), Institut de Chimie Moléculaire (FR 2769), Université Pierre et Marie Curie-Paris 6, 4 place Jussieu B. 229, 75005 Paris, France.

(1) Stuehr, D. J.; Griffith, O. W. In *Advances in Enzymology and Related Areas in Molecular Biology*; Meister, A., Ed.; Interscience: New York, 1992; Vol. 65, pp 287−346.
(2) Stuehr, D. J. *Biochim. Biophys. Acta* **1999**, *1411*, 217−230.
(3) Stuehr, D. J.; Santolini, J.; Wang, Z. Q.; Wei, C. C.; Adak, S. *J. Biol. Chem.* **2004**, *279*, 36167−36170.
(4) Groves, J. T.; Wang, C. C. Y. *Curr. Opin. Chem. Biol.* **2000**, *4*, 687−695.
(5) Rosen, G. M.; Tsai, P.; Pou, S. *Chem. Rev.* **2002**, *102*, 1191−1199.
(6) Stuehr, D. J.; Pou, S.; Rosen, G. M. *J. Biol. Chem.* **2001**, *276*, 14533−14536.
(7) Hurshman, A. R.; Krebs, C.; Edmondson, D. E.; Huynh, B. H.; Marletta, M. A. *Biochemistry* **1999**, *38*, 15689−15696.
(8) Wei, C. C.; Wang, Z. Q.; Wang, Q.; Meade, A. L.; Hemann, C.; Hille, R.; Stuehr, D. J. *J. Biol. Chem.* **2001**, *276*, 315−319.
(9) Wei, C. C.; Wang, Z. Q.; Hemann, C.; Hille, R.; Stuehr, D. J. *J. Biol. Chem.* **2003**, *278*, 46668−46673.
(10) Davydov, R.; Ledbetter-Rogers, A.; Martásek, P.; Larukhin, M.; Sono, M.; Dawson, J. H.; Masters, B. S. S.; Hoffman, B. M. *Biochemistry* **2002**, *41*, 10375−10381.
(11) Stone, K. L.; Behan, R. K.; Green, M. T. *Proc. Natl. Acad. Sci. U.S.A.* **2005**, *102*, 16563−16565.
(12) Kim, S. H.; Perera, R.; Hager, L. P.; Dawson, J. H.; Hoffman, B. M. *J. Am. Chem. Soc.* **2006**, *128*, 5598−5599.
(13) Ortiz de Montellano, P. R. In *Cytochrome P450*, 3rd ed.; Ortiz de Montellano, P. R.; Ed.; Kluwer Academic/Plenum Publishers: New York, 2005.
(14) Poulos, T. L. In *The Porphyrin Handbook*; Kadish, K. M., Smith, K. M., Guilard, R., Eds.; Academic Press: New York, 2000; Vol. 4, pp 189−218.

10.1021/ja066662r CCC: $37.00

species in the NOS reaction mechanism has yet to be experimentally verified. The actual observed intermediate immediately after $Fe^{III}-O_2^-$ in the first half-reaction is, in fact, the product Fe^{III} complex of the hydroxylated arginine (Scheme 1), indicating a fast substrate hydroxylation by the oxidizing species, presumably Cpd I.[8,10] The present paper addresses mechanisms of formation of this species and provides spectroscopic parameters for characterization of this elusive but nonetheless key species of NOS.

In most mechanistic proposals, two protons are required in order to cleave the O−O bond and form Cpd I and H_2O. These protons are believed to be supplied (from an unspecified source) to $Fe^{III}-O_2^{2-}$, *after the electron transfer* from H_4B to $Fe^{III}-O_2^-$, in order to assist in Cpd I formation.[3,8,18] Our study focuses on the question of when these protons are supplied, the timing of the H_4B radical appearance, and the consequences thereof for the ensuing reaction mechanism. Addressing this question is important since the knowledge of a correct protonation state (and hence charges) around the active site is critical to any future modeling studies of NOS. Moreover, our results will enable us also to characterize the hitherto unknown structure of NOS Cpd I vis-à-vis the known Cpd I structure of an another thiolate enzyme, chloroperoxidase (CPO),[11,12] and to establish thereby fundamental information for a key enzyme.

Methods

Definitions of the Quantum Mechanical System. Three guiding principles underlie our study. First, there is indirect evidence[10] that Cpd I, although still elusive, is formed in NOS, and this is also the current consensus. This provides the incentive to probe Cpd I formation in NOS. Second, as forming water is energetically much more favorable than having Cpd I and OH radical or OH^- anion, it is valid to assume that the distal oxygen atom of $Fe-O_2$ must acquire two protons from the surroundings in order to split the O−O bond and thereby form Cpd I and H_2O. Third, we assume that protons can be shuttled into the active site, since the active site location should be easily accessible to H_2O molecules, which are known to play a key role in O−O activation in other heme enzymes.[13,14,19] As will be shown below, this assumption was confirmed by our own molecular dynamics simulations. Thus, even though no obvious proton sources exist, other than the Arg substrate itself, water molecules are known to shuttle protons from the surface to the active site, e.g., in P450.[19] Other ways to add protons to the active site may come from the heme propionate arms, which remain mobile and can "fetch" protons from, for example, H_4B. Although the questions of the exact origin of the extra protons and their activation of the O−O bond remain elusive, as shall be seen, protons must be available in order to observe the $H_4B^{\bullet+}$ radical-cation and to complete the formation of Cpd I.

Computational Details. Calculations have been done within the hybrid quantum mechanical/molecular mechanical (QM/MM) scheme using the Chemshell[20] application combining Turbomole[21]/Jaguar[22] and DL-POLY.[20] The hybrid B3LYP[23−26] functional was used throughout this study for the QM part, and CHARMM[27] potentials were used for the MM part. Polarization of the QM layer by the MM layer is taken into account by inclusion of point charges in the framework of the charge-shift method.[28] QM/MM geometry optimization was done with Turbomole/DL-POLY using a double-ζ basis set (LACVP, as defined in Jaguar), where the QM region and the immediate vicinity in the MM region were allowed to move (see Supporting Information). QM/MM energy evaluations were done with the larger LACV3P*+ basis set by performing a Jaguar/DL-POLY single-point calculation on the optimized Turbomole/DL-POLY geometry. Spin and charge density values given in the text are taken from the LACV3P*+ calculations. Jaguar was used only for single-point QM/MM using a patch for Chemshell written in our laboratory (by E. Derat). To ensure that the Jaguar and Turbomole programs are compatible for the QM/MM calculations, comparisons were made on the same structures (**1R** and **1P**), showing that the generated energies were compatible within the Chemshell scheme (Table S0.1 in the Supporting Information).

Mössbauer Spectroscopic Calculations. To evaluate the Mössbauer parameters, the ORCA program[29] was used, and the Mössbauer parameters were obtained from single-point B3LYP calculations (at the geometries obtained after QM/MM optimization). The isomer shift was evaluated from the electron density at the iron nucleus.[30] Iron was described by the triply polarized core properties basis set CP(PPP),[30] and the other atoms were described by the SV(P) basis set[31] with the inner s-functions left uncontracted. For the iron atom, an enhanced integration grid was used, and the overall integration accuracy was increased to 7.[29] MM point charges were included in these calculations to probe the effect of the protein environment.

Models. Our models involve six reactions (reactions 1−6), starting from different reactant states and ending with Cpd I by means of protonating the O−O moiety. The initial structures were based on the published iNOS PDB,[18] which was solvated in a 16 Å layer of water, O_2 was added, and the system was further prepared according to standard procedures (see the Supporting Information). The QM part consists of 93−98 atoms, containing the porphine part of the heme with one propionate arm that hydrogen-bonds to H_4B, the thiolate ligand, O_2, H_4B, part of the substrate Arg, Arg375 which hydrogen-bonds to H_4B, and in some reactions one crystal water closest to the heme site (Scheme 2). All the structures in reactions 1−3 have been calculated at multiplicities 1, 3, 5, and 7, with a QM total charge ranging from 0 to +2. Reactions 4−6 were calculated at singlet states only. To elucidate the mechanism of Cpd I formation and the appearance of the H_4B radical before or after O_2 protonation, we explored a few putative reactions with different protonation states of the Arg substrate, the H_4B, and the O_2 molecule ligated to the heme (reactions 1−3 and tests of deproptonating H_4B; see below). In order to estimate the energetic cost of protonating our reactant species, another set of calculations was performed by extending the singlet reactant models to include as proton source the crystal water that forms a hydrogen bond to the Fe−[H]OO(H) moiety. The crystal water was taken as neutral and as a hydronium ion species (reactions 4−6). These reactions are described below.

Results

Molecular Dynamics Simulations. To investigate the changes in the environment over time, we performed a CHARMM molecular dynamics (MD) simulation for 300 ps using the PDB file obtained from the procedure described above, with the heme,

(15) Loew, G. H.; Harris, D. L. *Chem. Rev.* **2000**, *100*, 407−419.
(16) Meunier, B.; de Visser, S. P.; Shaik, S. *Chem. Rev.* **2004**, *104*, 3947−3980.
(17) Shaik, S.; Kumar, D.; de Visser, S. P.; Altun, A.; Thiel, W. *Chem. Rev.* **2005**, *105*, 2279−2328.
(18) Crane, B. R.; Arvai, A. S.; Ghosh, D. K.; Wu, C.; Getzoff, E. D.; Stuehr, D. J.; Tainer, J. A. *Science* **1998**, *279*, 2121−2126.
(19) Denisov, I. G.; Makris, T. M.; Sligar, S. G.; Schlichting, I. *Chem. Rev.* **2005**, *105*, 2253−2278.
(20) Chemshell 2.05b4, including DL-POLY: Sherwood, P.; et al. *J. Mol. Struct.: THEOCHEM* **2003**, *632*, 1−28.
(21) Ahlrichs, R.; Bär, M.; Häser, M.; Horn, H.; Kölmel, C. *Chem. Phys. Lett.* **1989**, *162*, 165−169.
(22) *Jaguar 5.5*; Schrodinger, LLC: Portland, OR, 2003.
(23) Lee, C.; Yang, W.; Parr, R. G. *Phys. Rev. B* **1988**, *37*, 785−789.
(24) Becke, A. D. *Phys. Rev. A* **1988**, *38*, 3098−3100.
(25) Becke, A. D. *J. Chem. Phys.* **1993**, *98*, 1372−1377.
(26) Becke, A. D. *J. Chem. Phys.* **1993**, *98*, 5648−5652.
(27) Brooks, B. R.; Bruccoleri, R. E.; Olafson, B. D.; States, D. J.; Swaminathan, S.; Karplus, M. *J. Comput. Chem.* **1983**, *4*, 187−217.
(28) Bakowies, D.; Thiel, W. *J. Phys. Chem.* **1996**, *100*, 10580−10594.
(29) Neese, F. *ORCA*, Version 2.4, Revision 10; Max-Planck-Institut für Bioanorganische Chemie: Mülheim a.d. Ruhr, Germany, 2004.
(30) Neese, F. *Inorg. Chim. Acta* **2002**, *337*, 181.
(31) Schäfer, A.; Horn, H.; Ahlrichs, R. *J. Chem. Phys.* **1992**, *97*, 2571.

Scheme 2. Schematic View of the QM Model Systems Used in the Calculations[a]

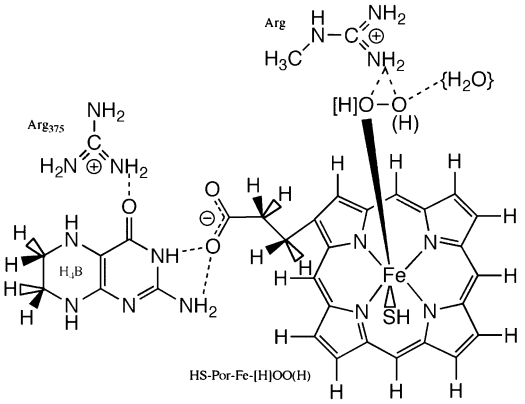

[a] The (H) proton is added in reaction 2, and both (H) and [H] protons are added in reaction 3. Reactions 4−6 contain $\{H_2O\}$.

O_2, Cys194, and outer solvent water layer (8−16 Å) being fixed. Figure 1 shows snapshots of the simulation at 0, 122, and 293 ps. At 0 ps (Figure 1a), only one of the water molecules is present in the region, a crystal water molecule already present in the original PDB file. The snapshot at 122 ps (Figure 1b) shows that this crystal water can be oriented differently with regard to O_2. Finally, at 293 ps (Figure 1c), a hydrogen-bonded network of a few solvent molecules has been created around the O−O moiety of the heme complex, due to the entrance of water molecules from the surface to the active site. The hydrogen-bonding network forms a connection to the solvent in the surface. This latter snapshot is then a "wet" pocket representation of the active site (see, e.g., discussions in refs 10 and 42), and this may be crucial for conduit of protons from the outside in. Interestingly, the pK_a of the Arg substrate in the "wet" site is 7.98 (calculated by PROPKA),[32] while when the 0 ps snapshot is used, it is 7.24. The unprocessed crystal structure PDB file (1NOD) yields a pK_a of 11.64. This demonstrates that H_2O molecules may very well "leak into" the active site, form hydrogen bond chains out to the surface, and affect the acidity of Arg, or of any potential proton donor other than Arg. Since the precise mechanism of protonation cannot be studied by QM/MM and requires extensive sampling of protonation states, the ensuing QM/MM calculations were started from the 0 ps snapshot.

QM/MM Calculations. To elucidate the protonation state at which the H_4B radical first appears, we explored three putative reactions, labeled as ***n*R → *n*P** (***n* = 1−3**; **R** and **P** are reactants and products). The respective reactants (**1R**, **2R**, **3R**) and products (**1P**, **2P**, **3P**) are shown in Figure 2 for the energetically lowest multiplicities of each species, together with valence electron orbital diagrams of each structure. The choice of the QM models is as described in the Methods section. In the first reaction (reaction 1, **1R → 1P**), no excess protons are present at the active site, and the formation of H_2O and Cpd I in **1P** requires the abstraction of two protons from the substrate Arg. The total system charge in this model is 0. In the second reaction (reaction 2, **2R → 2P**), one proton has been added to the distal oxygen of O_2 to form **2R** with a total system charge of +1. The third reaction (reaction 3, **3R → 3P**) adds yet another proton at the proximal oxygen position of O_2, leading to a total charge of +2. In all cases, the products include Cpd I and H_2O. The energies of the reactions are collected in Table 1, while spin densities are given in Table 2. (Many other details are given in the Supporting Information.)

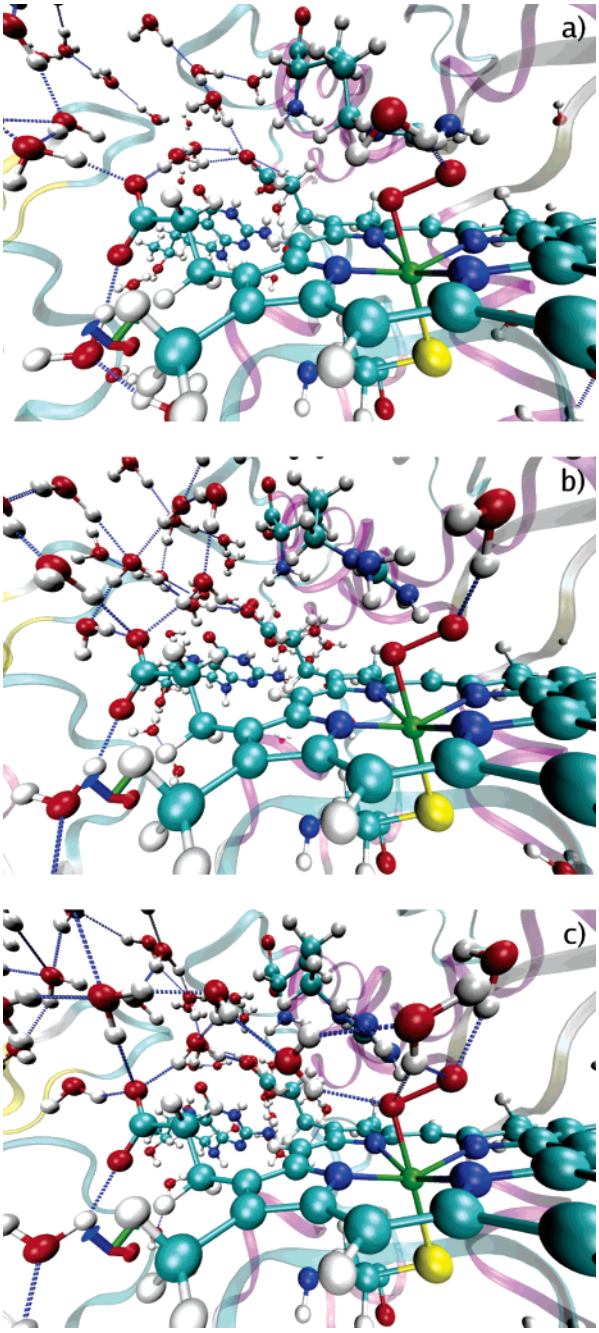

Figure 1. Three snapshots of MD run at (a) 0, (b) 122, and (c) 293 ps. The point-of-view is looking from the heme (foreground) toward the outside through the water channel. The substrate Arg is shown above O_2, and H_4B is visible in the background. Hydrogen bonds are highlighted in blue. The snapshots are discussed in the text.

Reaction 1. Inspection of Table 1 shows that the formation of Cpd I is endothermic, well over 20 kcal/mol, in all the four spin states. The reactant side (**1R**) consists of a singlet-state structure in the energetically lowest form, with two singly occupied valence orbitals with opposite spins, located one on the iron (π^*_{yz}) and the other on O_2 (π^*_{OO}). The Arg substrate is hydrogen-bonded to O_2 via its N$^{\omega}$-proton by 1.69 Å. With this electronic structure, this complex is still in the oxy form,

(32) Li, H.; Robertson, A. D.; Jensen, J. H. *Proteins* **2005**, *61*, 704−721.

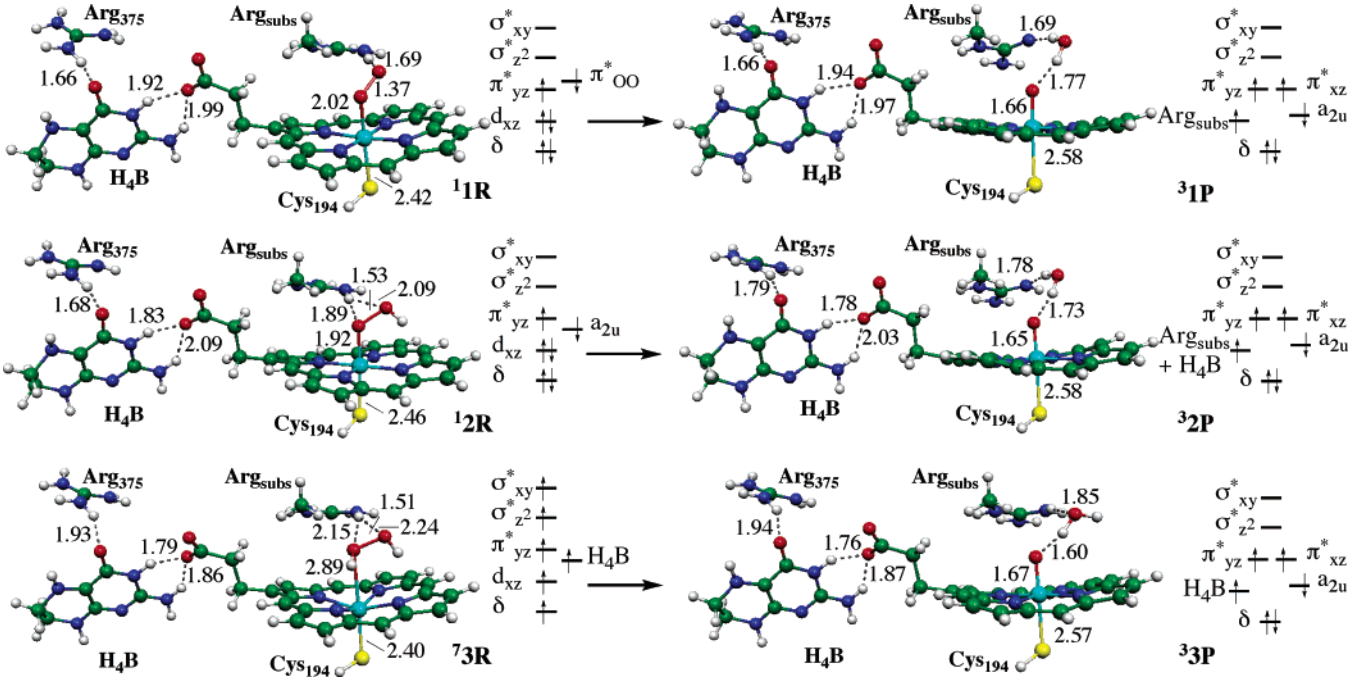

Figure 2. Structures of reactants (*n***R**) and products (*n***P**) for the three reactions investigated in this study. The geometric data correspond to the species with the energetically lowest multiplicity. The valence electron configurations are shown alongside the structures. All distances are in Å.

Table 1. Relative QM/MM Energies (in kcal/mol) for the Conversion of [HS−Por−Fe[H]OO(H)] (*n***R**) to Cpd I and Various Protonation States of Arg (*n***P**); ***i*** = **1**−**3**

	singlet[a]	triplet	quintet	septet
1R (Fe−OO)	**0.00**	1.61	1.39	1.06
1P (Arg−N•)	22.77	22.72	22.88	31.91
2R (Fe−OOH)	**0.00**	0.42	5.32	3.53
2P (Arg−NH)	13.83	12.40	14.29	25.47
3R (Fe−HOOH)	**0.00**	−3.45	−6.11	−6.22
3P (Arg−NH_2)$^+$	−25.65	−25.72	−25.32	−15.07

[a] The reactant structure of each reaction has been chosen as reference for the reaction (marked in bold). All the products contain also Cpd I in addition to the indicated species in each **P** entry.

Table 2. Excess Spin Density Distribution in the Ground States for the Species in the Reactions *n***R** → *n***P**[a]

	Fe	O_{inner}	O_{outer}	S_{Cys194}	Por	Arg_{subs}	H_4B
^{1}**1R**	1.15	−0.53	−0.48	−0.02	−0.10	−0.01	0.00
^{3}**1P**	1.38	0.79	0.01	−0.22	−0.94	0.98	0.00
^{1}**2R**	1.14	0.00	−0.01	−0.15	−0.92	0.00	−0.06
^{3}**2P**	1.40	0.77	0.01	−0.29	−0.51	0.21	0.43
^{7}**3R**	4.12	0.00	0.00	0.39	0.62	0.00	0.87
^{3}**3P**	1.52	0.67	0.01	−0.33	−0.81	0.00	0.94

[a] The left-hand superscript signifies the spin state of the species.

$Fe^{III}-O_2^-$. In accordance with this assignment, no electron transfer takes place from H_4B immediately after the O_2 binding to form the $Fe^{III}-O_2^{2-}$ complex, and indeed no spin is found on H_4B in **1R** in Table 2. On the product side (**1P**), the triplet-state structure is found to be nominally the lowest in energy, with the usual doublet $\pi^*_{xz}{}^1$ $\pi^*_{yz}{}^1$ $a_{2u}{}^1$ Cpd I valence orbital configuration[14−17] together with a radical in a p orbital on the doubly deprotonated N^{ω}-atom of substrate Arg. The lack of protons at the active site required an abstraction of both Arg N^{ω}-protons during the formation of H_2O, and the requisite excess electron needed for the process was provided by the deprotonated Arg. This and the fact that no electron transfer occurs from H_4B (Table 2) do not support the proposals that spontaneous electron transfer must take place from H_4B to O_2 upon binding of O_2 to the heme. Considering that the barriers leading to and from this structure are likely to be higher than the endothermicity of the reaction, this reaction pathway is ruled out.

Reaction 2. Here the reactant (**2R**) contains an additional proton to form an Fe−OOH moiety. However, this species, with the singly occupied π^*_{yz} orbital on the iron and the a_{2u} orbital on the porphyrin, is not Cpd 0, since it is still missing one electron in the porphyrin. As can be seen from Table 2, despite the addition of one proton, *H_4B still does not supply an electron to the heme moiety*. Attempts to obtain a Cpd 0 species starting from a wave function where the missing electron comes from H_4B (thus creating an $H_4B^{\bullet+}$ cation-radical) were not successful; the calculations always ended up with the current spin distribution as shown for **2R** in Table 2. It follows that addition of one proton to form Fe−OOH does not lead to Cpd 0 formation with concomitant creation of an $H_4B^{\bullet+}$ cation-radical. As such, in line with the cryogenic experiment in NOS,[10] we find no support for a Cpd 0 intermediate in the catalytic cycle of NOS, unlike in other heme enzymes where Cpd 0 is well known to exist.[14,19] While H_4B carries no spin on the reactant side, about half a spin is developed on it on the product side. Here, one proton has been taken from the Arg substrate to form H_2O, creating a moderate amount of spin on Arg as well. The reaction itself is endothermic, but three of the states do not reach the 17 kcal/mol mark, calculated to be an approximate upper limit on the basis of the measured enzyme kinetics and the Eyring equation.[33] Thus, tentatively and provided that the barriers are not too much higher, these states may still be within the plausible limit. The overall assessment of reaction 2 is that, while the reaction is plausible, the relatively high energy of the product combined with a moderate development of the H_4B spin makes the reaction

(33) Cho, K.-B.; Gauld, J. W. *J. Phys. Chem. B* **2005**, *109*, 23706−23714.

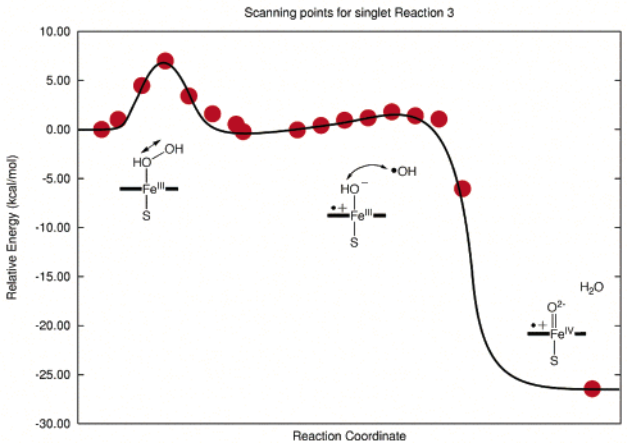

Figure 3. QM/MM energy scanning points from **3R** to formation of **3P**, using the LACVP basis set. Except for the ground states, each scan point is optimized with loose convergence criteria in the interest of saving time. The arrows show the scanned distance parameter between the steps. All calculations were done in the singlet state ($H_4B^{\bullet+}$ radical-cation coupled to a doublet heme moiety).

less compatible with experiments and would be best classified as a "borderline case". Moreover, the fact that the $H_4B^{\bullet+}$ cation-radical has been observed experimentally even without the Arg substrate[7] is a strong indication that the spin should be entirely on H_4B.

Reaction 3. Here, the reactants (**3R**) involve the ferric−hydrogen peroxide complex, $Fe^{III}-H_2O_2$. The Fe−O bond is weak, and the ground state for this heme−H_2O_2 complex species is therefore a septet state with six unpaired valence electrons: five on $Fe^{III}-H_2O_2$ and one full spin on H_4B. It can be seen from Table 2 that the $H_4B^{\bullet+}$ cation-radical formation corresponds to an electron transfer from H_4B to assist the formation of H_2O_2, thus corresponding in principle to a proton-coupled electron transfer (PCET) mechanism, where the electron and proton are supplied by different sources. The lowest state at the product side is a triplet state (the ground state of Cpd I is the doublet state coupled into a triplet state to the radical on H_4B), lying more than 10 kcal/mol lower in energy than the septet product. Hence, a spin-state crossover has to occur during this reaction to produce Cpd I. In contrast to the above two model reactions, this one is exothermic. Clearly, therefore, when the two protons are supplied from external sources (not from the Arg substrate), the process is exothermic and the $H_4B^{\bullet+}$ cation-radical appears.

The final feature of reaction 3 is the formation of Cpd I from Fe−HOOH by a rather unusual mechanism, shown in Figure 3. Thus, the scan from Fe−HOOH to Cpd I + H_2O exhibits an initial homolytic O−O bond breaking coupled with internal electron transfer (to form porphyrin cation-radical) and hydrogen abstraction of the proximal H by the departing OH radical. All in all, therefore, this process leads to heterolytic cleavage of the O−O bond and formation of Cpd I by a novel mechanism. Once again, this mechanism implies that the intermediacy of Fe−OOH (Cpd 0) is not necessary for the formation of Cpd I, since there seems to be a low-energy path directly from Fe−HOOH.

Addition of two protons to the distal oxygen in the singlet state generated an alternative **3R′** structure, Fe−O−OH_2 that was 20.2 kcal/mol above **3R**, 8.5 kcal/mol of the excess energy deriving from the QM region (see Supporting Information). This

Scheme 3. Schematic Picture of H_4B Hydrogen Bonded to One of the Heme Propionate Arms

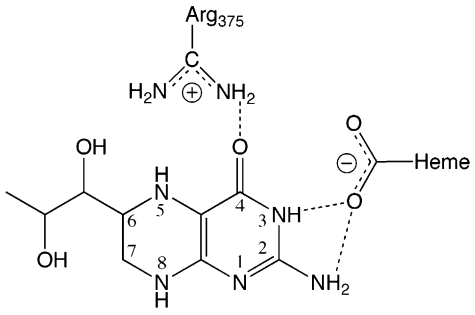

is in line with the very high energy (>20 kcal/mol) found in a recent QM/MM calculation of O−O activation in P450.[34] The Fe−OOH_2 species possesses one excess spin in π^*_{yz}, and an additional one is delocalized between the a_{2u} orbital and H_4B, thus showing a valence electron configuration consistent with an intermediate in the reaction **2R** → **3R′** → **3P**. Due to its higher energy, however, the **3R′** structure was not pursued any further. At the same time, it should be emphasized that, as long as two protons are added, the result is formation of Cpd I and water and the appearance of a radical $H_4B^{\bullet+}$ in an exothermic process, as in the net **3R** → **3P** process.

Mechanistic Impact of the Protonation State of H_4B. Since reactions 1 and 2 showed that deprotonation of Arg is not favorable, we investigated the potential of H_4B as the proton source for all three reactions. As can be seen from Scheme 3, due to the hydrogen bond that exists between the heme propionate group and the N3-hydrogen of H_4B, there is a possibility that H_4B may get deprotonated by the carboxylate group in the process, and after electron transfer will form a neutral radical rather than a cation-radical. Indeed, some studies have suggested that this would be the case,[35,36] while other experimental studies favor the cation-radical model.[37,38]

Using the singlet structures of each of the six species presented in this study, the N3-proton was shifted to the carboxylate group and then optimized. However, in all of the structures, no such stable state was found. Instead, the proton returned to H_4B during the optimizations. In an attempt to keep the proton with the carboxylate, the O−H distances were held frozen at 0.95 Å. This constraint resulted in structures that were anywhere from 14 to 55 kcal/mol higher in energy (LACVP energies) than the corresponding $H_4B^{\bullet+}$ cation-radical structures (Table S4.3). The only significant changes to the spin distribution were in reaction 2 (Table S4.2), where half a spin developed in **2R** and a full spin in **2P**, but again, these states were significantly higher in energy than the ones listed in Table 1. Hence, within our QM/MM scheme, the scenario involving deprotonation of the N3-proton and the creation of a neutral H_4B radical is not supported. Our study does not, however, treat the cases where H_4B is initially protonated (to H_5B^+)[10] or when it binds to the enzyme with the N5-proton either deprotonated

(34) Zheng, J.; Wang. D.; Thiel, W.; Shaik, S. *J. Am. Chem. Soc.* **2006**, *128*, 13204−13215.
(35) Morao, I.; Periyasamy, G.; Hillier, I. H.; Joule, J. A. *Chem. Commun.* **2006**, 3525−3527.
(36) Crane, B. R.; Arvai, A. S.; Ghosh, S.; Getzoff, E. D.; Stuehr, D. J.; Tainer, J. A. *Biochemistry* **2000**, *39*, 4608−4621.
(37) Schmidt, P. P.; Lange, R.; Gorren, A. C. F.; Werner, E. R.; Mayer, B.; Andersson, K. K. *J. Biol. Inorg. Chem.* **2001**, *6*, 151−158.
(38) Du, M.; Yeh, H.-C.; Berka, V.; Wang, L.-H.; Tsai, A. L. *J. Biol. Chem.* **2003**, *278*, 6002−6011.

Table 3. Energetics (in kcal/mol) for Reactions 4, 5, and 6

reaction	reactant		(intermediate)		product
4	**1R** + H_2O		→		**2R**$^-$ + OH$^\bullet$
	0.00				40.71
5	**1R** + H_3O^+	→	**2R** + H_2O	→	**3R** + OH$^\bullet$
	33.76		0.00		53.39
6	**2R** + H_3O^+		→		**3R** + H_2O
	34.40				0.00

Table 4. Calculated Mössbauer Data for NOS Cpd I and Experimental Values for CPO Cpd I

	η	ΔE_Q (mm/s)	δ (mm/s)
1P	0.115	1.019	0.12
2P	0.081	1.064	0.10
3P	0.195	1.294	0.09
CPO (exp)[a]	n/a	1.02	0.14

[a] Data from ref 40.

or missing altogether, a case that has been postulated as another possibility to generate the H_4B radical.[39]

The Role of Water Deprotonation on the Energetic of 1R and 2R. In order to investigate the feasibility of protonating **1R** and **2R** to yield **2R** and **3R**, respectively, we extended the models to include the nearby crystal water that is hydrogen-bonded to the O_2 moiety. Specifically, we studied the three new processes, reactions 4−6, as described below. All the calculations were done on singlet states, and the energetic results are summarized in Table 3.

Reaction 4. This reaction is formally **1R** + H_2O → **2R**$^{(-1-Z)}$ + OH^Z, where Z defines the charge; in the case of $Z = -1$, the reaction forms **2R** and OH^-, while in the case of $Z = 0$, the reaction leads to **2R**$^-$ and OH$^\bullet$. As we found, however, in this reaction and in the next one, formation of an OH$^\bullet$ radical was always preferred over production of OH^-, and the water molecule could not be used as a source of protons. The first entry in Table 3 shows that "protonating" **1R** by H_2O is highly endothermic. Furthermore, as we noted, this is not actually a protonation process, but rather an H-atom transfer, since the reaction leads to an OH$^\bullet$ radical. All efforts to swap an electron and generate an OH^- species led back to a wave function that corresponds to the OH$^\bullet$ radical. Due to the H$^\bullet$ transfer, the resulting Fe−OOH species in **2R** is Cpd 0, *but it forms at an energetic cost of more than 40 kcal/mol*. As such, the H-atom transfer reaction from water can be ruled out, and since the OH^- state is even less stable than the OH$^\bullet$, a direct proton abstraction from water is ruled out, too. We therefore studied in parallel also protonations by H_3O^+ in the next reaction.

Reaction 5. In this reaction we studied both the protonation of **1R** by H_3O^+ and that of **2R** by water, **1R** + H_3O^+ → **2R** + H_2O → **3R**$^-$ + OH$^\bullet$. The use of H_3O^+ stands to reason, considering that the source of the proton more likely comes from the bulk solution, where *excess* protons are available. Hence, the first part of reaction 5 describes H_3O^+ protonating **1R** to form **2R** (second entry of Table 3). The process is, in fact, spontaneous, and in order to obtain the energy of the H_3O^+ + **1R** species, we had to keep the O−H$^+$ distance fixed at 1.0 Å, or else the proton moves automatically over to the O_2 moiety during the optimization. In the follow-up step of reaction 5, we attempted to transfer a proton from H_2O to **2R**. As can be seen in Table 3, this process is endothermic by 53.4 kcal/mol and again generates an OH$^\bullet$ radical along with **3R**$^-$. Since the H-atom transfer supplies an electron to the heme, now no $H_4B^{\bullet+}$ radical-cation is formed, making the reaction further incompatible with experiment and once again ruling out water as a protonating species.

Reaction 6. Here, we calculated the protonation energy of **2R** by H_3O^+, **2R** + H_3O^+ → **3R** + H_2O. This is seen to be exothermic by 34.4 kcal/mol, using the same 1.0 Å constraint as in reaction 5 to obtain the energy of H_3O^+ + **2R**. Now, in addition to **3R**, there appears a radical-cation $H_4B^{\bullet+}$. Incidentally, the structure for H_3O^+ + **2R** involves a hydrogen bond between H_3O^+ and the distal oxygen of the Fe−OOH (**2R**) moiety, presumably setting up for a formation of the alternate high-energy species Fe−OOH_2 (**3R′**) as described earlier instead of the lower Fe−HOOH (**3R**). This is of no consequence to the conclusions, however, as the exothermicity of this reaction is still clearly greater than the energy difference between the two **3R**'s (20.2 kcal/mol).

Comparisons of NOS Cpd I with Known Cpd I Species. The spin density on the S_{cys194} ligand of NOS Cpd I is seen from Table 2 to be approximately 0.3, in reasonable accord with the recent spin density assignment in CPO (0.23).[12] The Fe−O and Fe−S bond lengths in Figure 2 are seen to be also in reasonable agreement with the recent EXAFS values for CPO Cpd I of 1.65 and 2.48 Å, respectively.[11]

The calculated Mössbauer isomer shift, quadrupole splitting, and asymmetry parameters for the three models of triplet Cpd I of NOS are given in Table 4, alongside the corresponding experimental data for CPO.[40] The data obtained for **3P** are different from the data obtained for **1P** and **2P**. These two latter species have parameters similar to the experimental values of CPO Cpd I. The differences between them are, however, large enough to be potentially observable.

Comparing the NOS Cpd I to other theoretical studies, similar features are seen. Our Fe−S bond length values of 2.58, 2.58, and 2.57 Å for **1P**, **2P**, and **3P** triplet (doublet, if only Cpd I is considered) structures, respectively, are in good agreement with the value of 2.592 Å obtained with QM/MM on cytochrome $P450_{cam}$ using comparable models and basis sets.[41] The same agreement can be seen for the Fe−O distance as well (1.66, 1.65, and 1.67 Å vs 1.653 Å). The spin distributions are similar, too, where the combined FeO (2.17, 2.17, and 2.19 vs 2.177) and S_{Cys} (−0.22, −0.29, and −0.33 vs −0.270) spin densities are in reasonable agreement. The spin density on the porhyrin (−0.94, −0.51, and −0.81 vs −0.915) differs substantially when it comes to the Cpd I species in the ^{3}**2P** structure, a result that can be seen to originate in radical delocalization between the porphyrin, substrate Arg, and H_4B.

Discussion

The protonation state of the NOS active site, including O_2 and H_4B, is a subject of mechanistic importance that has so far generated quite a few puzzles. Considering the stoichiometries in Scheme 1, it is inevitable to have to account for the two extra protons that must enter the system at some point. By comparing the reaction energies of reactions 1−3, we are led

(39) Menyhárd, D. K. *Chem. Phys. Lett.* **2004**, *392*, 439−443.

(40) Rutter, R.; Hager, L. P.; Dhonau, H.; Hendrich, M.; Valentine, M.; Debrunner, P. G. *Biochemistry* **1984**, *23*, 6809−6816.

(41) Schöneboom, J. C.; Lin, H.; Reuter, N.; Thiel, W.; Cohen, S.; Ogliaro, F.; Shaik, S. *J. Am. Chem. Soc.* **2002**, *124*, 8142−8151.

to two key conclusions: (a) the protons most likely have to be supplied *before* H_4B turns into a radical-cation, and (b) the source of proton is external.

Conclusion (a) originates in reaction 3, which shows that *only* when two such protons are supplied, the $H_4B^{\bullet+}$ radical-cation appears along with a reasonably low-energy mechanism that generates Cpd I. Conclusion (b) arises from the fact that reactions 1 and 2 show that using Arg as a proton source leads to endothermic reactions. Since the use of H_4B as the proton source (via the N3-position) was also found to be unlikely, the proton source should be external. At the same time, our MD simulations (Figure 1) show, in accord with previous postulates,[10,42] that water can access the active site, thus providing a pathway of supplying the protons from the surface/bulk into the active site. Reactions 4−6 were carried out to have a better assessment of whether the source of protons is water or hydronium ions. The results of reaction 4 and the reaction **5I** → **5P** clearly rule out the possibility that a water molecule by itself can be the proton source; the cost of the process is energetically too high, and the process leads to $OH^{\bullet}$ instead of OH^- (Table 3). By contrast, the reaction **5R** → **5I** and reaction 6 demonstrate that a more realistic modeling of the proton source should be H_3O^+ (presumably shuttled from the bulk water). In this case, the protonation process is exothermic and the $H_4B^{\bullet+}$ species appears, thus showing that protonation from bulk solvent should be possible without any excessive energy penalties.

Our modeling of the external proton source as H_3O^+, while not ideal, reasonably assumes that such a proton shuttle is possible in NOS, via a Grotthaus mechanism, since the active site is accessible to the outside solvent (Figure 1c), and since H_3O^+ ions exist in the bulk near the surface. A full study would require, however, sampling of protonation states of the protein and of the water molecules in order to properly address how this excess proton is transferred from the bulk/surface via a chain of water molecules to the active site. Such a study of the protonation mechanism with bulk solvent is beyond our means and beyond the scope of the paper. Thus, this paper demonstrates a principle: *when protons are available, the $H_4B^{\bullet+}$ radical-cation appears and subsequently Cpd I is generated.*

Concerning the presence of Cpd I in the first half-reaction, our study shows that Cpd I (**3P**) can certainly be made from **3R** as a starting point (Figure 3), in a process that is exothermic and does not involve excessive barriers. Future calculations will address the issue of whether Cpd I can catalyze the NHA formation as well. In addition, we note that the **1R** and **3R** species, calculated here, are also possible sources of the observed productions of free $O_2^{\bullet-}$ and H_2O_2, respectively.[43,44] Although H_2O_2 may derive also from $O_2^{\bullet-}$, our results are compatible with proposals that there is a separate production of H_2O_2 as well.[6] It should, however, be pointed out that our results regarding reaction 3 do not at all imply that the NOS process can be short-circuited by using H_2O_2 instead of O_2, as is also found experimentally.[45] In our proposal, the $Fe^{III}-H_2O_2$ complex appears along with an electron transfer from H_4B and is quickly transformed to Cpd I and water. In addition, our preliminary calculations show that H_2O_2 binding to Fe^{III} in NOS by itself *is not an exothermic process*, but is either thermoneutral or slightly endothermic (data not shown).

Finally, our study reveals a novel mechanism of O−O bond heterolysis and formation of Cpd I, directly from the Fe−HOOH complex, with an estimated energy barrier of around 13 kcal/mol or less (estimated as a 6 kcal/mol spin-flip from septet to singlet, followed by a 7 kcal/mol barrier, as shown in Figure 3). This, in turn, means that Cpd 0 may not be an essential intermediate in the cycle, in conformity with the cryo-annealing results, where this species was not seen for NOS.[10] However, the cryo-annealing experiments independently generated an $Fe^{III}-O_2^{2-}$ species by γ-irradiation at 77 K, while subsequent annealing to 165 K was found to be sufficient to convert the species to the ferric complex of the hydroxylated arginine. This is in contrast to $P450_{cam}$, where Cpd 0 appears with the addition of an electron to the oxyferrous complex already at 77 K, and the reaction continues only after annealing to above 210 K. This different behavior in NOS did not absolutely rule out that non-accumulating Cpd 0 is an intermediate in the process, but the authors[10] interpreted the results to signify that proton(s) could be abstracted from elsewhere in the pocket than the substrate. The same conclusion was reached from a recent study of eNOS crystal structures with CO or NO bound.[42] This interpretation matches our results that protons do not originate in the substrate and that Cpd 0 really is not essential to the formation of Cpd I. As such, while we cannot absolutely and conclusively rule out reaction 2, our calculations suggest that, in order for the NOS cycle to proceed forward, *a simultaneous double protonation of O_2 could be taking place after binding to Fe^{II}.*

Conclusions

The results in this paper show that the availability of protons is a *prerequisite* for the NOS reaction to progress beyond the $Fe^{III}-O_2^-$ intermediate, since H_4B electron transfer transpires only when the active site is doubly protonated. Calculations show that protonation from the bulk solvent should be possible, and once the heme is protonated to form Fe−HOOH, the $H_4B^{\bullet+}$ radical-cation species appears. The reaction can then occur in a facile manner through cleavage of the O−O bond and hydrogen abstraction from Fe−OH by $^{\bullet}OH$ to form H_2O and Cpd I (Figure 3). The Mössbauer data show that Cpd I species **3P**, where H_4B is itself a radical, is significantly different than **1P** and **2P**, which are also formed via endothermic pathways. These parameters may help the eventual characterization of NOS Cpd I species by experiment.

Acknowledgment. The research is supported by the Israel Science Foundation (ISF). The paper is dedicated to the memory of Edgar Heilbronner.

Supporting Information Available: Computational procedures, *xyz* coordinates, energies of the various species, and complete ref 20. This material is available free of charge via the Internet at http://pubs.acs.org.

JA066662R

(42) Li, H.; Igarashi, J.; Jamal, J.; Yang, W.; Poulos, T. L. *J. Biol. Inorg. Chem.* **2006**, *11*, 753−768.
(43) Pou, S.; Pou, W. S.; Bredt, D. S.; Snyder, S. H.; Rosen, G. M. *J. Biol. Chem.* **1992**, *267*, 24173−24176.
(44) Heinzel, B.; John, M.; Klatt, P.; Bohme, E.; Mayer, B. *Biochem. J.* **1992**, *281*, 627−630.
(45) Pufahl, R. A.; Wishnok, J. S.; Marletta, M. A. *Biochemistry* **1995**, *34*, 1930−1941.